Ultrathin Anisotropic Films Assembled from Individual Single-Walled Carbon Nanotubes and Amine Polymers

Nina I. Kovtyukhova*,†,‡ and Thomas E. Mallouk†

Department of Chemistry, The Pennsylvania State University, University Park, Pennsylvania 16802, and Institute of Surface Chemistry, N.A.S.U., 17, General Naumov Street, 03680 Kiev, Ukraine

Received: September 20, 2004; In Final Form: November 5, 2004

Oxidized individual single-walled carbon nanotubes and amine polymers have been assembled into 11−32-nm-thick well-ordered conductive films. The films show highly anisotropic electrical conductivity, which is dominated by the nanotubes in the horizontal plane and by polymer-mediated tunneling in the vertical direction. The ratio of the "along" to "across" conductivity is $\sim 10^3$. The subnanometer thick polymer layers interleaved with monolayers of nanotubes show conductivity several orders of magnitude higher than films of pristine polymers.

Introduction

In light of inevitable scaling down of electronic circuits, carbon nanotubes (CNT) have emerged as a unique material for use in chemically assembled nanoscale devices.[1] Logic gates[1a,b] and highly sensitive molecular sensors[1g] have been fabricated using a selected rope or individual tube as a single device, which, however, requires sophisticated techniques for nanotube selection and manipulation. On the other hand, significant advances have been made in the fabrication of larger-scale devices (e.g., network transistors,[2a] LEDs,[2b,c] photovoltaic devices,[2d] printable conductors[2e]) from composite nanotube networks and films containing polymers, including biologically active macromolecules.[2f] This approach is technologically simple and compatible with the processing methods envisioned for low-cost flexible electronics.[2a,e] CNT−polymer devices are usually prepared using either single-walled nanotube (SWNT) ropes or multiwalled nanotubes (MWNT).[2,3] Because of the relatively large diameter and micrometer-scale length of these nanotube blocks, the resulting composite films are rough and thick. Also, reliable control of components alignment and dispersion within the films remains a challenge, which to a certain extent makes it difficult to determine the charge transport mechanism in hybrid CNT−polymer structures. The enhanced electronic conductivity of the composite versus pure polymer films is primarily ascribed to spontaneously formed nanotube percolation networks, although CNTs can also act as hole-injectors[2c] and dopants[2g,h] within the polymer films. An important potential advantage of composite nanotube−polymer devices is the possibility of combining the electronic properties of both of the components. To fully realize this, the controllable separation of CNT and polymer phases within a single device structure can be useful.[2d]

To exploit the power of the CNT−polymer composite devices at the low end of the nanometer-size regime, there is thus a need for ultrathin well-organized films with controllable structure, morphology, and electronic properties. Key requirements here are the availability of relatively monodisperse solutions of short and thin CNTs, and nanotube wall functionalization, which enables reliable control over the interfacial chemistry of the components. Recently, we reported homogeneous aqueous dispersions of individual single-walled carbon nanotubes, which were prepared by oxidative exfoliation and shortening of the SWNT ropes.[4] These oxidized nanotubes (SWNTox) contain significant amounts of oxygen functionalities on their ends and walls and, therefore, bear negative surface charge and form very stable aqueous sols and conductive dense films.

Here, we report the electrical properties of ordered SWNTox/polymer films with thicknesses close to or less than the diameter of an average SWNT rope. The films show highly anisotropic conductivity, which is dominated by the polymer component in the direction perpendicular to the film surface, while the conductivity in the plane of the film is dominated by SWNTs. This has been achieved by controllable insertion of nanometer-thick nanotube monolayers between very thin polymer layers. We also demonstrate that the conductivity of the polymers can be increased by several orders of magnitude when they are assembled in subnanometer thick layers interleaved with layers of SWNTox. SWNTox-polyaniline (PAN) and SWNTox-polyethylenimine (PEI) films are grown using the layer-by-layer assembly technique (LBL), which is a simple route to organized films from oppositely charged components,[5] including SWNT ropes.[3]

Experimental Section

Materials. Aqueous sols of individual single-walled carbon nanotubes (SWNTox) were prepared by complete oxidative exfoliation of SWNT ropes (provided by Tubes@Rice) as described previously.[4] Also, the characterization of SWNTox by HRTEM, AFM, XRD, Raman, EELS, XPS, FTIR, UV−Vis−near-IR methods, and electrical measurements has been reported.[4] Briefly, the SWNTox sols, which are used in this study, are stable for the period of months and contain only individual SWNTs of 40−500 nm in length and 0.8−2 nm in diameter. No noticeable amount of SWNT bundles was found. The SWNTox contain carboxyl, hydroxyl, and carbonyl groups on their ends and walls (average C:O ratio is 2.7, but it is suggested to be higher on the walls and lower on the ends). When adsorbed onto the positively charged surfaces, these nanotubes readily form fairly densely packed films. The

* Corresponding author. E-mail: nina@chem.psu.edu.
† The Pennsylvania State University.
‡ Institute of Surface Chemistry.

10.1021/jp045725u CCC: $30.25
Published on Web 01/22/2005

SWNTox films reveal ohmic current−voltage behavior, although their conductivity is ~3 orders of magnitude lower than that of nonoxidized SWNTs.

PEI (linear, M_n ca. 423) and poly(acrylic acid) PAA were purchased from Aldrich and used as 1 wt % aqueous solutions. Deionized water was used in all experiments. The emeraldine base form of polyaniline (PAN) was prepared as described by Chiang and MacDiarmid[6] and was used as a 0.015 wt % solution in *N*,*N*-dimethyl formamide (DMF). DMF (99.9+%, HPLC grade, evaporation residue <0.0005%) was purchased from Aldrich.

Au-coated glass slides (purchased from EMF) were cleaned by washing with hexane, methanol, and water. p-Si(100)/SiO_2-(1 μm) wafers (purchased from University Wafer) and glass substrates were sonicated in hexane, washed with methanol and water, and then cleaned (20 min) with "piranha" solution (4:1 concentrated H_2SO_4:30% H_2O_2. **Caution**: "piranha" solution reacts violently with organic compounds.) and rinsed thoroughly with water.

Synthesis of Multilayer Films. The multilayer SWNTox/polymer films were prepared by the conventional layer-by-layer assembly technique. Briefly, a substrate was alternately immersed in a solution of polymer and SWNTox (0.4 g/L) for 15 min. As we have previously shown,[4] the adsorption times longer than 5 min are necessary to ensure a densely packed nanotube monolayer (see an AFM image below). When adsorption times of 1−2 min were applied, separated individual SWNTs randomly distributed on the surface were found. After each adsorption step, the substrate was rinsed with water (or DMF for PAN) and dried in an Ar stream. Multilayer SWNTox/polymer films were grown by repeating this two-step adsorption cycle.

Characterization. Ellipsometric measurements were made with a Gaertner model L2W26D ellipsometer. The analyzing wavelength was 632 nm (SWNTox absorption is negligible at this wavelength), the incident angle was 70°, and the polarizer was set at 45°. Au and Si refractive indices were determined from blank samples. The refractive index of SWNTox films was approximated as $N_f = 1.540$. X-ray photoelectron spectra (XPS) were recorded with Kratos Analytical Axis Ultra: monochromatic Al, spot-size 700−350 μm, X-ray power 280 W, takeoff angle 90°. The spectra were curve-fitted using the CasaXPS program (Casa Software Ltd.). IR transmission and UV−Vis−near-IR absorption spectra were obtained using Perkin-Elmer 1600 Series FTIR and Perkin-Elmer Lambda 900 instruments, respectively. For both spectroscopic measurements, the films were prepared by drop-casting a solution onto AgCl or glass slides and drying in a vacuum for 14+ h at ambient temperature. Atomic force microscopy was performed with a Digital Instruments Nanoscope IIIa in tapping mode using a 3045 JVW piezo tube scanner.

For electrical measurements, films were deposited on a p-Si(100)/SiO_2(1 μm) substrate with lithographically prepared 200-nm-thick Au pads. The $(PEI/SWNTox)_{15}PEI$, $(PAN/SWNTox)_{19}PAN$, and $(PAN/PAA)_{15}PAN$ films were deposited by the layer-by-layer method, and films of pure PAN, PEI, and SWNTox were drop-cast from the starting solutions and dried in air. Prior to measurement, all samples were dried in a vacuum for 1 h. I−V characteristics along the film were measured between two neighboring Au-pads (device area 100 × 100 μm^2 or 50 × 100 μm^2). For measurements across the film, Ag electrodes were lithographically predefined and evaporated on the top of the film so that they crossed the bottom Au-electrode at a right angle (device area 3 × 3 μm^2). The measurements were performed in dry air at ambient temperature with a HP 4156B Precision Semiconductor Parameter Analyzer.

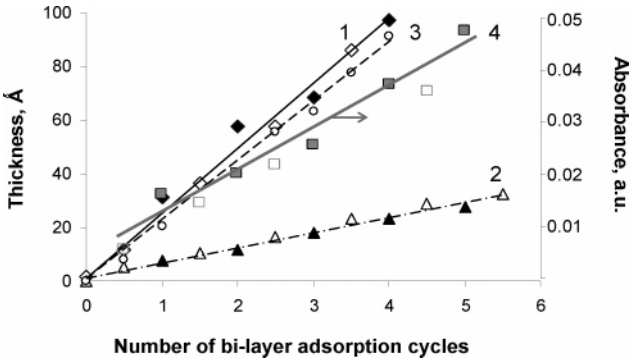

Figure 1. Plots of ellipsometric thickness (1−3) and absorbance at $\lambda = 500$ nm (4) versus number of adsorption cycles for multilayer PEI/SWNTox (1, 4), PAN/SWNTox (2), and PAN/PAA (3) films deposited on Au (1−3) and glass (4) substrates. Solid dots indicate SWNTox-terminated surfaces.

Results and Discussion

Film Growth. Ellipsometric measurements show linear film growth on Au (Figure 1) and Si/SiO_2 substrates, which implies that approximately equal amounts of the components are deposited in each bi-layer cycle. In the case of $Au(PEI/SWNTox)_4$ films (Figure 1, tr.1), the average thickness of the nanotube layers is about 1.5 nm, which falls within the range (0.8−2 nm) of diameters of SWNTox.[4] Thinner SWNTox/PEI films grow on the Si/SiO_2 substrate; however, on both of the substrates, SWNTox/PEI multilayers grow considerably thicker than SWNTox/PAN films (Figure 1, tr.2), which suggests weaker SWNTox interaction with PAN than with PEI. Ellipsometric thicknesses of both kinds of SWNTox/polymer films are in agreement with thicknesses measured by AFM. The similar packing density of SWNTox in each monolayer is also confirmed by monitoring light absorbance at $\lambda = 500$ nm (PEI does not absorb at this wavelength) during the LBL deposition of a multilayer PEI/SWNTox film on a glass substrate (Figure 1, tr.4). The graph shows a linear absorbance increase with each deposited SWNTox monolayer, and the glass slide gradually acquires a dark-brown color characteristic for the SWNTox sol. Also, no significant absorbance decrease, and hence desorption of SWNTox, is observed in the following PEI deposition cycles (Figure 1, tr.4, □).

Because LBL deposition is a sequential adsorption technique, the extent of film growth in each cycle as well as the structural organization and electrical properties of the resulting multilayer film strongly depend on the strength of interactions between components in the adjoining layers. Therefore, a significant part of this study is focused on examining polymer−SWNTox interactions by XPS, FTIR, and UV−Vis−near-IR spectroscopic methods.

XPS and IR Spectroscopy. In the XPS spectra, the sharp and symmetrical N 1s peak (399.1 eV) in the starting PEI (inset in Figure 2a), which is characteristic of the amine C−N bonds, changes when the polymer is assembled in the multilayer SWNTox/PEI film (Figure 2a). Three higher binding energy components arise in the spectrum of multilayer SWNTox/PEI films, which are consistent with the presence of N−C═O (400.1 eV), $C-NH_3^+$ (401.3 eV), and $C-NH_2^+-C$ (402.2 eV) groups.[7] In the C 1s core level spectrum of the SWNTox/PEI film (Figure 2b), the presence of the C 1s peaks of SWNTox[4] and of the starting PEI (285.6 eV, see inset in Figure 2b) is clearly seen.

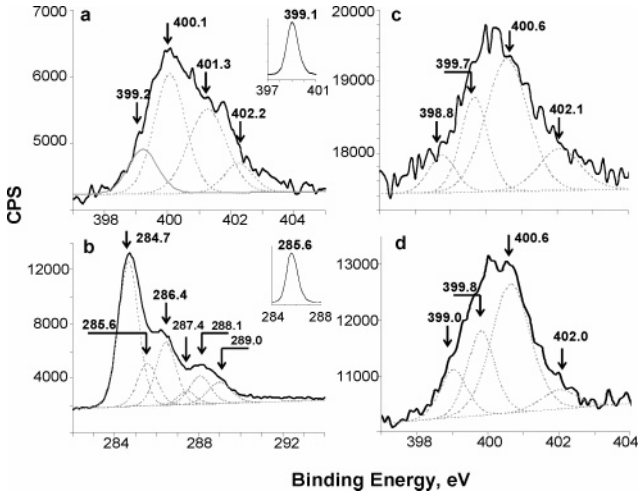

Figure 2. N1s (a, c, d) and C1s (b) core level X-ray photoelectron spectra (XPS) of multilayer SWNTox/polymer films (a−c) and pure PAN (d): (a, b) Au(PEI/SWNTox)$_{15}$PEI; (c) Au(PAN/SWNTox)$_5$PAN; (d) PAN film drop-cast on Au substrate from 0.015 wt % solution in DMF. Insets in (a) and (b) show N1s and C1s spectra, respectively, of PEI film drop-cast on Au substrate from 4% aqueous solution.

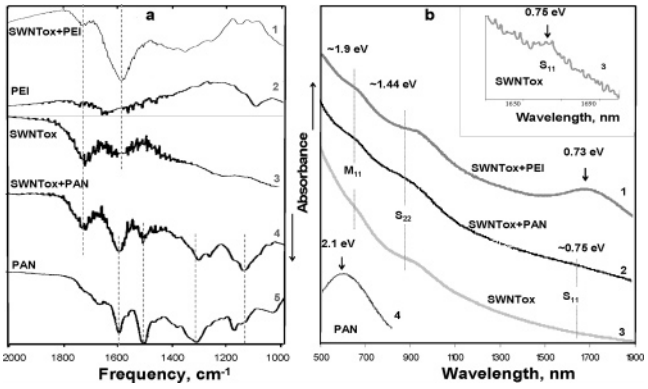

Figure 3. (a) FTIR transmission spectra of SWNTox+PEI (1), PEI (2), SWNTox (3), SWNTox+PAN (4), and PAN (5) films. b) UV−vis−near-IR absorption spectra of SWNTox+PEI (1), SWNTox+PAN (2), SWNTox (3), and PAN (4) films. The inset shows details of the SWNTox spectrum. SWNTox+PEI, a blend (1:1) of aqueous SWNTox (0.4 g/L) and PEI (0.01%) solutions; PEI, 0.01 wt % aqueous solution; SWNTox, 0.4 g/L aqueous sol; SWNTox+PAN, a blend (1:1) of SWNTox (0.4 g/L) and PAN (0.015 wt %) solutions in DMF; PAN, 0.015 wt % solution in DMF.

However, the contribution of amine C−N bonds (285.6 eV) is considerably decreased, and a peak which may be assigned to amide N−C═O bonds (288.1 eV) is observed. The latter peak was not found in the C 1s core level spectrum of the starting SWNTox.[4]

FTIR spectroscopy shows similar differences between a SWNTox+PEI film and the individual components (Figure 3a, sp.1−3). A set of new absorption bands appearing in the range of 1000−1700 cm^{-1} (Figure 3a, sp.1) implies the formation of covalent bonds and resembles the IR spectrum of organic amides.[8,9] The band at about 1260 cm^{-1} may be assigned to the C−N stretching vibrations in amides. The intensity ratio of bands centered at about 1730 and 1584 cm^{-1} changes dramatically as compared to the SWNTox spectrum. The band at 1584 cm^{-1} becomes considerably more intense and wider, which indicates the superposition of several bands. The C═O stretching modes of deprotonated carboxyl groups of SWNTox, the bending modes of N−H bonds in neutral and protonated amine groups in PEI (Figure 3a, sp.2), and the $\nu_{C=O}$ and δ_{N-H} vibrations of amides may contribute to this band. An IR spectrum similar to this one was reported for SWNTs modified with tetradecylaniline through the formation of amide moieties.[10]

While ionic carboxyl−amine interactions are expected for SWNTox assembly with amine polymers, appearance of new peaks in the XPS and IR spectra of the SWNTox/PEI films cannot be adequately interpreted in terms of only electrostatic interaction. The formation of other bonds is evident. To study the possibility of covalent bond formation in a simpler model system, we prepared aqueous blends of SWNTox with propylamine (PA) and dipropylamine (DPA), and then treated them with NaOH to ion-exchange the amines. The initial and alkali-treated blends were drop-cast onto CaF_2 or AgCl slides and dried in a vacuum for 16 h to remove the unreacted and exchanged PA and DPA. FTIR spectra of the initial SWNTox+PA and SWNTox+DPA blends (not shown) are almost identical to the SWNTox+PEI spectrum (Figure 3a, trace 1). In the spectra of the NaOH-treated blends, one can still see bands in the ranges of 2960−2840 cm^{-1} (ν_{C-H}), 1280−1240 cm^{-1}, and a band at 1144 cm^{-1}, which are present in the spectra of the untreated blends. Upon treatment with NaOH, the carboxyl-related vibrations at 1770−1700 cm^{-1} disappear, but broad bands centered at 1579 cm^{-1} (for DPA) and 1588 cm^{-1} (for PA) with shoulders at 1630−1680 cm^{-1} are still present. The shape and position of these bands suggest that besides the SWNTox carboxylate groups other groups may exist. Because the N−H deformation bands of neutral and protonated amines (PA and DPA) are expected to vanish after treatment with NaOH, it is reasonable to suggest contributions from $\nu_{C=O}$ and δ_{N-H} vibrations of amides or $\nu_{C=N}$ vibrations of imine groups. The imines, however, do not appear in the XPS spectra of the multilayer SWNTox/PEI film, and hence their formation is less likely. In either case, the fact that some amount of PA and DPA molecules remain bound to SWNTox after treatment with NaOH establishes that covalent interactions of the aliphatic amines with SWNTox functionalities are possible under these conditions. This may shed some light on the SWNTox−PEI interactions as well. For example, in the spectrum of the NaOH-treated SWNTox+PA blend, the band at 1588 cm^{-1} is much more pronounced than that in the SWNTox DPA spectrum, which implies that the PEI terminal primary amine groups may be more reactive toward the SWNTox carboxyl groups.

In contrast to the SWNTox−PEI system, absorption bands in the FTIR spectrum of a SWNTox+PAN blend (Figure 3a, sp.4) may be interpreted as the superposition of bands appearing in the spectra of the individual components. The main difference between the PAN (Figure 3a, sp.5) and SWNTox+PAN spectra is seen in the C−H bending vibrations of the quinoid ring:[11] a band centered at 1310 cm^{-1} shifts to 1299 cm^{-1}, and the band at 1140 cm^{-1} becomes more intense in the SWNTox−PAN spectrum. A less pronounced difference is also observed between N 1s XPS spectra of the multilayer SWNTox/PAN and PAN films (Figure 2c,d). Both of the envelopes can be fitted with four components characteristic of the PAN emeraldine state:[12] neutral imine C═N−C (398.8−399.0 eV), neutral amine C−NH−C (399.7−399.8 eV), and protonated amine (400.6 eV) and imine (402.0−402.1 eV) groups. The intensity ratio of the protonated to neutral amine groups is almost the same in both spectra, which allows one to rule out a condensation reaction for neutral amine groups. However, the intensity ratio of the protonated to neutral imine bonds in the SWNTox/PAN spectrum is approximately 3 times that in the spectrum of PAN. These data suggest that ionic interactions between the protonated imine and amine nitrogens and SWNTox carboxyl groups do

SCHEME 1

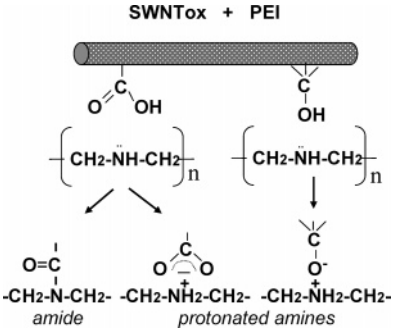

SCHEME 2

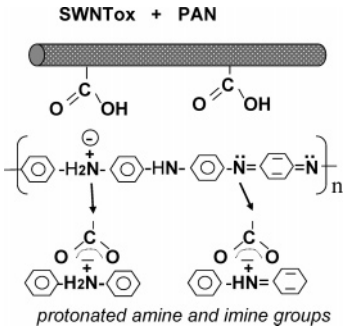

occur. The important role of the carboxyl groups is indirectly confirmed by the growth of thicker PAN multilayers with polyacrilic acid (PAA), which has a higher density of carboxyl groups (Figure 1, tr.3) than SWNTox. Because the PAN benzenoid-amine and quinoid-imine groups are considerably less basic than the PEI alkylamines, weaker ionic interactions are expected between the neighboring SWNTox and PAN layers. The probable types of interactions between SWNTox and PEI and PAN are illustrated in Schemes 1 and 2.

UV−Vis−Near-IR Spectroscopy. We also examined the possibility of charge-transfer complex formation in the SWNTox−PAN systems suggested by other groups.[13,14] An absorption band at 2.1 eV, which is found in the UV−vis−near-IR spectrum of PAN (Figure 3b, sp.4) and is characteristic for the PAN emeraldine state, does not appear in the SWNTox+PAN spectrum. This "exciton" band has been ascribed to electronic transitions between the highest occupied energy level centered on the benzenoid rings and the lowest unoccupied energy level centered on the quinoid rings.[15] Quenching of this absorbance by interaction with SWNTox may result either from depletion of the "benzenoid band" or from filling of the "quinoid band". However, IR and XPS data suggest that the imine-quinoid units are most strongly affected. By analogy with the interaction of aromatic hydrocarbons with the basal plane of graphite,[16] and the sidewalls of carbon nanotubes,[14] we postulate the formation of charge-transfer complexes between the π-systems of SWNTox and PAN.

Comparing UV−vis−near-IR spectra of SWNTox+PEI and SWNTox films (Figure 3b, sp.1,3), we find that interaction with PEI causes a considerable increase in the intensity of peaks assigned to the interband transitions between the first (S_{11}) and second (S_{22}) sets of density of states singularities of the semiconducting nanotubes (Figure 3b, sp.1,3). This is particularly evident for the S_{11} peak, which is also shifted ~0.02 eV to lower energy relative to SWNTox (see inset in Figure 3b). As we previously showed,[4] SWNTox contains a significant amount of sp^3-hybridized carbon atoms inserted into the sidewalls, which leads to lower intensities of the S_{11}, S_{22}, and M_{11} peaks relative to unoxidized SWNTs. This change in electronic structure can be explained by partial depletion of the valence band of the semiconducting nanotubes.[17,18] The increased intensity and lower-energy shift of the S_{11} peak resulting from the interaction with PEI suggest some refilling of the valence band.[17] This may be caused by deprotonation of the SWNTox carboxyl and hydroxyl groups and negative charging of the nanotubes in the basic PEI solution. A similar suggestion was made by Zhao et al. to explain the gradual intensity increase of the S_{11} peak with an increase in pH.[19] Our observation that significantly less basic PAN does not noticeably affect the intensity of the interband transitions of the semiconducting nanotubes (Figure 3b, sp.2,3) is consistent with their findings.

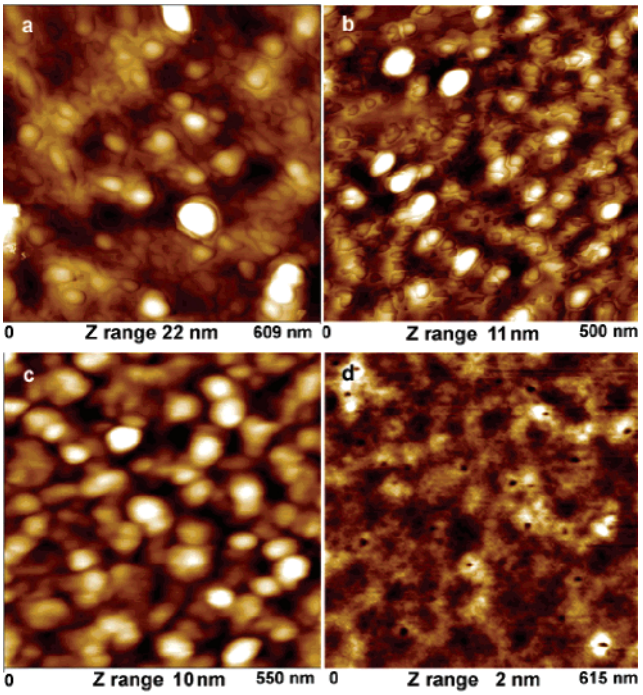

Figure 4. Tapping mode AFM images of the films layer-by-layer deposited on Au (a−c) and Si/SiO_2 (d) substrates. (a) $Au(PEI/SWNTox)_4$; (b) $Au(PAN/SWNTox)_5PAN$; (c) $Au(PAN/PAA)_4$; (d) $Si/SiO_2/SWNTox$: the substrate was primed with aminobutyldimethylmethoxysilane; the 15 min adsorption cycle was followed by rinsing with water and drying in an Ar stream.

The XPS, FTIR, and UV−vis−near-IR data show that the polymer−SWNTox interaction in the multilayer films is complex and involves the formation of several bond types. While Coulomb attraction between the oppositely charged components is the long-range driving force in the films assembly, additionally, the formation of covalent bonds (in the case of PEI) and charge-transfer complexes (in the case of PAN) becomes possible between closely packed SWNTox and polymers in the neighboring layers.

AFM. AFM images of the $Au(PEI/SWNTox)_4$ and $Au(PAN/SWNTox)_5PAN$ films (Figure 4) are relatively featureless and give an average roughness in the range of 2.3−1.3 nm, which is comparable to the range of SWNTox diameters. The $Au(PEI/SWNTox)_4$ film shows denser packing (Figure 4a) consistent with the ellipsometry data. The morphology of the SWNTox monolayers (Figure 4d) suggests the formation of ~1.5 nm-thick dense network of the nanotubes, which are in so close contact that individual features are undistinguishable. Such morphology is typical for the SWNTox monolayers prepared using adsorption times longer than 5 min[4] and is expected to enable good conductance of the SWNTox monolayers. The morphologies of both multilayer films (Figure 4a,b)

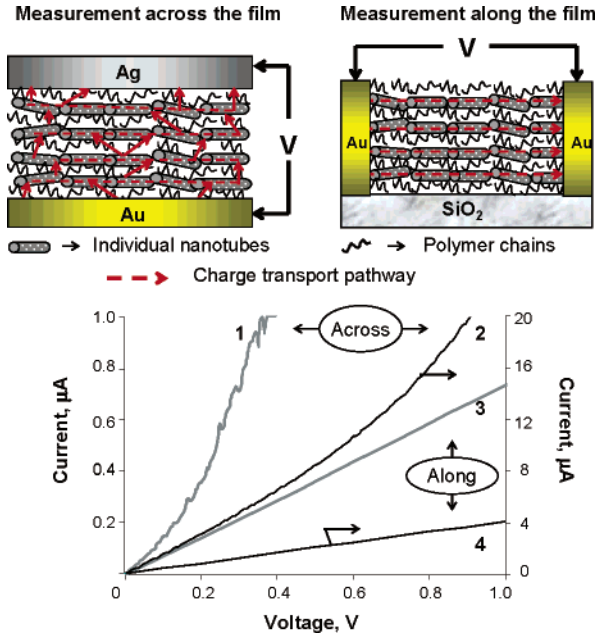

Figure 5. Top: Schematic representation of the multilayer SWNTox/polymer film structure and electrode positioning for electrical measurements across (left) and along (right) the films. Red arrows indicate charge pathways through the films. Bottom: I−V characteristics of Au-(PAN/SWNTox)$_{19}$PAN/Ag (1, 3) and Au(PEI/SWNTox)$_{15}$ PEI/Ag (2, 4) thin film devices measured across (1, 2) and along (3, 4) the films.

resemble that of the SWNTox monolayer (Figure 4d) and differ from the morphology of the Au(PAN/PAA)$_4$ films (Figure 4c). This suggests that SWNTox lateral organization in the monolayers mainly determines the multilayer structure and that the polymer chains are extended along the nanotube network.

Electrical Properties. Conductivity measurements were performed across and along the multilayer SWNTox/polymer films as shown schematically in Figure 5 (top). For both (PEI/SWNTox)$_{15}$PEI and (PAN/SWNTox)$_{19}$PAN films, I−V characteristics measured across the films are nonlinear with breakdown voltages in the range of ±(0.5−1) V, while the characteristics measured along the films show ohmic behavior in the voltage range of ±10 V (Figure 5). The ratio of the "across" to "along" resistivities ($\rho_\perp/\rho_{||}$) is ∼10^3 for each film (Table 1). These data suggest that the conductivity along the films is dominated by metallic nanotubes of the SWNTox layers, while the polymer layers contribute to the resistivity measured across the films as resistors connected in series (see scheme in Figure 5). The resistivities of the SWNTox and polymer layers in the films were estimated at roughly 0.5 and 1.7 Ω cm for SWNTox in the multilayers with PEI and PAN, respectively, 10^3−10^4 Ω cm for PEI, and 10^4−10^5 Ω cm for PAN (Table 1). Comparing these results to resistivities of the pure components shows that: (i) in the (PEI/SWNTox)$_{15}$PEI film, the SWNTox resistivity is similar to that of pristine SWNTox, and the PEI resistivity is ∼6 orders of magnitude lower than that of pure PEI; (ii) in the(PAN/SWNTox)$_{19}$PAN film, the SWNTox resistivity is ∼3.5 times that of the pure SWNTox film, and the PAN resistivity is 2−3 orders of magnitude lower than that of the PAN film.

The conductivity data are consistent with the idea that the packing density of the SWNTox monolayers in the PEI/SWNTox films is higher than that in the PAN/SWNTox films and is close to that of the pure SWNTox films.[4] It also should be noted that reproducible ohmic I−V behavior along the (PAN/SWNTox)$_{19}$PAN film is observed for 2−3 times shorter distances between the electrodes as compared to the (PEI/SWNTox)$_{15}$PEI film, which implies smaller lateral size of well-organized domains in the former. Both conclusions are consistent with the ellipsometry data. The considerably higher conductivity of the PEI and PAN assembled in the multilayer films relative to the pure polymers is an interesting finding. While the 3−4 orders of magnitude increase in conductance of CNT-PAN composite films has now been reported by several groups (see, e.g., ref 2e,i), it mainly resulted from the formation of nanotube percolation networks. In our case, this increase cannot be explained by the existence of random electrical contacts between neighboring SWNTox layers or some intermingling of nanotubes in the polymer monolayers. Both of these factors would lead to linear I−V characteristics and are more likely to be found in the more poorly organized PAN/SWNTox film, which, however, is less conductive. Polymer−SWNTox interactions along the nanotube walls may enable more parallel chain orientation and/or better lateral packing in the polymer monolayers than in the pure polymer films. In the case of PAN, doping by SWNTox acidic carboxyl groups may also improve the polymer conductivity. Some support for this idea can be found in the 1-order-of-magnitude decrease in resistivity of the multilayer (PAN/PAA)$_{15}$PAN film as compared to the pure PAN film (Table 1). An increase in the PAN conductivity has also been reported for composite PAN-MWNT films.[2h] However, the UV−vis−NIR spectrum of SWNTox+PAN film does not provide noticeable evidence for the formation of a more conductive PAN redox form.

It is also important to note that in the very thin polymer layers sandwiched between the conductive SWNTox layers, there is a high probability that an electron can transfer to the nanotube faster than it is localized by chain defect sites. The formation of covalent bonds (for PEI) or charge-transfer complexes (for PAN) should enhance electronic coupling between the polymers

TABLE 1: Electrical Resistivity of the SWNTox/Polymer and Polymer Films Measured Across and Along the Films

	across the film			along the film		
film	film thickness[a] (nm)	$\rho_{\perp film}$ (Ω cm)	$\rho_{polymerlayer}$[c] (Ω cm)	film thickness[a] (nm)	$\rho_{\|\|film}$ (Ω cm)	$\rho_{SWNToxlayer}$[c] (Ω cm)
Au(PEI/SWNTox)$_{15}$PEI/Ag	32 ± 1	2.8 ± 1 × 10^3	10^3−10^4	22 ± 1	0.9 ± 0.4	0.5
Au(PAN/SWNTox)$_{19}$PAN/Ag	11 ± 0.8	2.5 ± 2 × 10^4	10^4−10^5	14 ± 0.8	3.6	1.7
Au/SWNTox/Ag	58 ± 4	0.35 ± 0.1		58 ± 4	0.35 ± 0.1	
Au/PEI/Ag	∼12	10^{10}−10^{11}				
Au/PAN/Ag	∼15	6 × 10^7				
Au(PAN/PAA)$_{15}$PAN/Ag	32 ± 0.7	3 × 10^6		27 ± 0.7	∼10^{13} [b]	
Si/SiO$_2$ substrate				n/a	∼10^{13} [b]	

[a] Film thickness was estimated by ellipsometry and AFM and corrected for the roughness measured by AFM. [b] Resistance, Ω. [c] Resistivity of PEI and PAN in the multilayer films was determined as $\rho_{polymer} = \rho_\perp L_f/L_p$, where L_f is the thickness of the film and L_p is the sum of thicknesses of the polymer monolayers. SWNTox resistivity in the multilayer films was determined as $\rho_{SWNTox} = \rho_{||} L_{SWNTox}/L_f$, where L_{SWNTox} is the sum of thicknesses of the SWNTox monolayers in the film. All thicknesses were estimated by ellipsometry.

and nanotubes. Surprisingly, lower resistivity is found for the single layers of insulating PEI than for layers of semiconducting PAN (Table 1). Although the transport mechanism in these multilayer systems is not well understood, it seems reasonable that electron transfer occurs by tunneling through the polymer chains with a relatively small number of the repeat units between the electrical contacts and that SWNTox/PEI covalent-bond contacts provide higher conductivity. It has been shown that the chemical bonding between organic SAMs and metal or semiconductor electrodes dramatically increases electronic coupling (see, for review, ref 20 and references therein). An alternative transport mechanism, which is operative in thin films of metal nanoparticles cross-linked with organic molecules,[21] involves activated hopping between nearest electron-rich neighbors. This mechanism implies a decrease in conductivity with increasing interparticle distance (in our case, SWNTox layers) because of the exponential decay of the tunneling probability and contradicts our experimental results which show higher conductivity through the thicker PEI versus PAN layers.

Conclusions

Oxidized individual SWNTs have been assembled layer-by-layer with amine polymers into well-ordered conductive ultrathin films. Lateral and vertical film organization reveals itself in highly anisotropic conductivity, which is dominated by the metallic nanotubes in the horizontal plane and by polymer-mediated tunneling in the vertical direction. Although LBL assembly has been routinely used to combine a wide variety of building blocks with very different electrical conductivity, the strongly pronounced anisotropy in LBL-derived structures is rather unique. It is the small size and strong adhesion to each other of the SWNTox blocks[4] that enables their good lateral organization within the ultrathin dense and conductive monolayers. The subnanometer thick polymer layers interleaved with the layers of SWNTox show conductivity several orders of magnitude higher than films of pristine polymers. To our knowledge, such a strong increase in conductivity of the polymer component has not been found in other types of CNT−polymer composites. Even though conductance of the reported composites is quite high, it is basically assigned to the nanotube percolation networks. This finding should allow one to considerably extend the range of polymers, including insulating ones, that can be explored for potential nanoscale electronics and sensing applications. Because short individual nanotubes with uniform diameters of molecular size are used, the resulting SWNTox/polymer films are thin and smooth enough to be integrated as p-type conductive layers into nanometer-sized electronic devices, such as nanowire diodes.[22] It should also be interesting to use SWNTox for the fabrication of carbon-derived structures for testing and exploiting the electronic properties of individual organic molecules. Such structures would preclude the formation of metal nanofilaments across the molecular gap, which have been invoked as the cause of switching effects in some metal/molecule/metal junctions.[23]

Acknowledgment. We thank Vince Bojan and the Penn State Materials Characterization Lab for performing XPS measurements. We are also grateful to Prof. T. N. Jackson and C.-C. S. Kuo for their assistance with the electrical measurements. We thank Tubes@Rice for the supply of nanotubes. This work was supported by the NSF (grant CHE-0095394).

References and Notes

(1) (a) Rueckes, T.; Kim, K.; Joselevich, E.; Tseng, E.; Cheung, C.-L.; Lieber, C. M. *Science* **2000**, *289*, 94. (b) Bachtold, A.; Hadley, P.; Nakanishi, T.; Dekker, C. *Science* **2001**, *294*, 1317. (c) Bockrath, M.; Cobden, D.; McEuen, P.; Chopra, N.; Zettl, A.; Thess, A.; Smalley, R. *Science* **1997**, *275*, 1922. (d) Avouris, P. *Acc. Chem. Res.* **2002**, *35*, 1026. (e) Henk, W.; Postma, C.; Teepen, T.; Yao, Z.; Grifoni, M.; Dekker, C. *Science* **2001**, *293*, 76. (f) Javey, A.; Kim, H.; Brink, M.; Wang, Q.; Ural, A.; Guo, J.; McIntyre, P.; McEuen, P.; Lundstrom, M.; Dai, H. *Nat. Mater.* **2002**, *1*, 241. (g) Kong, J.; Franklin, N.; Zhou, C.; Chapline, M.; Peng, S.; Cho, K.; Dai, H. *Science* **2000**, *287*, 622.

(2) (a) Bradley, K.; Gabriel, J.; Gruner, G. *Nano Lett.* **2003**, *3*, 1353. (b) Curran, S.; Ajayan, P.; Blau, W.; Carroll, D.; Coleman, J.; Dalton, A.; Davey, A.; Drury, A.; McCarthy, B.; Maier, S.; Strevens, A. *Adv. Mater.* **1998**, *10*, 1091. (c) Kim, J.; Kim, M.; Choi, J. *Synth. Met.* **2003**, *139*, 565. (d) Ago, H.; Petritsch, K.; Shaffer, M.; Windle, A.; Friend, R. *Adv. Mater.* **1999**, *11*, 1281. (e) Blanchet, G.; Fincher, C.; Gao, F. *Appl. Phys. Lett.* **2003**, *82*, 1290. (f) Zheng, M.; Jagota, A.; Starno, M.; Santos, A.; Barone, P.; Chou, S.; Diner, B.; Dresselhaus, M.; Mclean, R.; Onoa, G.; Samsonidze, G.; Semke, E.; Usrey, M.; Walls, D. *Science* **2003**, *302*, 1545. (g) Chen, G.; Shaffer, M.; Coleby, D.; Dixon, G.; Zhou, W.; Fray, D.; Windle, A. *Adv. Mater.* **2000**, *12*, 522. (h) Zengin, H.; Zhou, W.; Jin, J.; Czerw, R.; Smith, D.; Echegoyen, L.; Carroll, D.; Foulger, S.; Ballato, J. *Adv. Mater.* **2002**, *14*, 1480. (i) Blanchet, G. B.; Subramoney, S.; Bailey, R. K.; Jaycox, G. D.; Nuckolls, C. *Appl. Phys. Lett.* **2004**, *85*, 828.

(3) (a) Mamedov, A.; Kotov, N.; Prato, M.; Guldi, D.; Wisksted, J.; Hirsch, A. *Nat. Mater.* **2002**, *1*, 190. (b) Rouse, J.; Lillehei, P. *Nano Lett.* **2003**, *3*, 59.

(4) Kovtyukhova, N.; Mallouk, T.; Pan, L.; Dickey, E. *J. Am. Chem. Soc.* **2003**, *125*, 9761.

(5) (a) Decher, G. *Science* **1997**, *277*, 1232. (b) Mallouk, T.; Kim, H.; Ollivier, P.; Keller, S. In *Comprehensive Supramolecular Chemistry*; Alberti, G., Bein, T., Eds.; Elsevier: Oxford 1996; Vol. 7, p 189. (c) Fendler, J. *Chem. Mater.* **1996**, *8*, 1616.

(6) Chiang, J.; MacDiarmid, A. *Synth. Met.* **1986**, *13*, 13.

(7) Beamson, G.; Briggs, D. *High-resolution XPS of organic polymers: the Scienta ESCA300 database*; Wiley: Chichester, New York, 1992.

(8) *The Aldrich library of FT-IR spectra*; Sigma-Aldrich Co.: MO, 1997; Vol. 1.

(9) We note that for comparative purposes the FTIR spectrum of starting PEI was recorded using a drop of very diluted (0.01 wt %) aqueous PEI, and therefore the intensity typical for PEI bands in the frequency range of 1000−1500 cm^{-1} is very low. This makes us believe that the strong absorption bands within this range appearing in the spectrum of SWNTox+PEI film prepared with the same amount of PEI may indicate the amide formation.

(10) Hamon, M.; Chen, J.; Hu, H.; Chen, Y.; Itkis, M.; Rao, A.; Eklund, P.; Haddon, R. *Adv. Mater.* **1999**, *11*, 834.

(11) Quillard, S.; Louarn, G.; Lefrant, S.; MacDiarmid, A. *Phys. Rev. B* **1994**, *50*, 12496.

(12) Monkman, A.; Stevens, G.; Bloor, D. *J. Phys. D* **1991**, *24*, 738.

(13) Sun, Y.; Wilson, S.; Schuster, D. *J. Am. Chem. Soc.* **2001**, *123*, 5348.

(14) (a) Star, A.; Stoddart, J.; Steuerman, D.; Diehl, M.; Boukai, A.; Wong, E.; Yang, X.; Chung, S.; Choi, H.; Heath, J. *Angew. Chem., Int. Ed.* **2001**, *40*, 1721. (b) Chen, R.; Zhang, Y.; Wang, D.; Dai, H. *J. Am. Chem. Soc.* **2001**, *123*, 3838.

(15) McCall, R.; Ginder, J.; Leng, J.; Ye, H.; Manohar, S.; Masters, J.; Asturias, G.; MacDiarmid, A.; Epstein, A. *Phys. Rev. B* **1990**, *41*, 5202.

(16) (a) Jaegfeldt, H.; Kuwana, T.; Johansson, G. *J. Am. Chem. Soc.* **1983**, *105*, 1805. (b) Castillejos-Lopez, E.; Nevskaia, D.; Munoz, V.; Rodriguez-Ramos, I.; Guerrero-Ruiz, A. *Langmuir* **2004**, *20*, 1013.

(17) Itkis, M.; Niyogi, S.; Meng, M.; Hamon, M.; Hu, H.; Haddon, R. *Nano Lett.* **2002**, *2*, 155.

(18) Chen, J.; Hamon, M.; Hu, H.; Chen, Y.; Rao, A.; Eklund, P.; Haddon, R. *Science* **1999**, *282*, 95.

(19) Zhao, W.; Song, C.; Pehrsson, P. *J. Am. Chem. Soc.* **2002**, *124*, 12418.

(20) Cahen, D.; Hodes, G. *Adv. Mater.* **2002**, *14*, 789.

(21) Feldstein, M.; Keating, C.; Liau, Y.; Natan, M.; Scherer, N. *J. Am. Chem. Soc.* **1997**, *119*, 6638.

(22) Kovtyukhova, N.; Mallouk, T. *Adv. Mater.*, in press.

(23) Service, R. *Science* **2003**, *302*, 556.